



## Life cycle assessment of electric traction induction machines

Downloaded from: <https://research.chalmers.se>, 2026-04-14 13:59 UTC

Citation for the original published paper (version of record):

Hsieh, M., Nordelöf, A., Grunditz, E. et al (2026). Life cycle assessment of electric traction induction machines. *International Journal of Life Cycle Assessment*, 31(1-3).

<http://dx.doi.org/10.1007/s11367-026-02610-7>

N.B. When citing this work, cite the original published paper.



# Life cycle assessment of electric traction induction machines

Meng-Ju Hsieh<sup>1</sup> · Anders Nordelöf<sup>2,3</sup> · Emma Grunditz<sup>1</sup> · Torbjörn Thiringer<sup>1</sup>

Received: 12 June 2025 / Accepted: 19 October 2025  
© The Author(s) 2026

## Abstract

**Purpose** Geopolitical challenges, coupled with the expected surge in demand for electric vehicles (EVs), may create uncertainties in the supply of rare-earth elements (REEs) used in permanent magnet synchronous machines (PMSMs), the predominant type of electric traction machine (e-machine) in EVs. This life cycle assessment (LCA) study benchmarks an REE-free alternative machine type, induction machine (IM), against a classic PMSM with REE magnets for EV application.

**Materials and methods** Three IM variants are evaluated: one with copper (Cu) stator windings and Cu rotor bars, one with Cu stator windings and aluminum (Al) rotor bars, and one with Al stator windings and Al rotor bars. Beyond a baseline setup, the study also explores strategies to reduce GHGs, including using green virgin Al and enhancing the material utilization rate during the punching process for electrical steel sheets, referred to as a “green manufacturing” route. Furthermore, a sensitivity analysis of GHGs on magnet production is also conducted.

**Results and discussion** The results show that the PMSM causes the least greenhouse gas (GHG) emissions due to its higher power density and efficiency. In contrast, the IMs with Al conductors exhibit lower environmental impacts in the categories of toxicity and acidification compared to those with (more) copper. The sensitivity analysis shows that IMs have the potential to display lower carbon footprints than PMSMs under favorable conditions. The research highlights the environmental trade-offs in e-machine design for EVs.

**Conclusions** The study underscores the need for a sustainable perspective on e-machine materials and manufacturing processes. It demonstrates that REE-free IMs, particularly when paired with green manufacturing strategies, can be competitive alternatives to PMSMs in terms of environmental performance, depending on design and production choices.

## Highlights

- Compares rare-earth-free induction machines with permanent magnet machines.
- Aluminum-based induction machines show lower toxicity and acidification.
- Green manufacturing and material choices reduce greenhouse gas emissions.
- Sensitivity analysis shows induction machines can have lower carbon footprints.
- Highlights environmental trade-offs in electric machine design for vehicles.

**Keywords** Life cycle assessment (LCA) · Electrification · Electric vehicle · Induction machine (IM) · Rare-earth-element-free

---

Communicated by Xin Sun

---

✉ Meng-Ju Hsieh  
mengju.hsieh@chalmers.se

Anders Nordelöf  
anders.nordelof@chalmers.se; anders.nordelof@vti.se

Emma Grunditz  
emma.grunditz@chalmers.se

Torbjörn Thiringer  
torbjorn.thiringer@chalmers.se

<sup>1</sup> Division of Electric Power Engineering, Chalmers University of Technology, Gothenburg 412 96, Sweden

<sup>2</sup> Division of Environmental Systems Analysis, Chalmers University of Technology, Gothenburg 412 96, Sweden

<sup>3</sup> The Swedish National Road and Transport Research Institute, Regnbågsgatan 1, Gothenburg 417 55, Sweden

## 1 Introduction

To ease the situation of greenhouse gas (GHG) emissions caused by the transportation sector, the electrification of vehicles is strongly promoted by actors such as IPCC (2023) and IEA (2023c). In response, given that charging duration and driving range of electric vehicles (EVs) are key factors influencing consumer purchase decisions and thus EV adoption (Forsythe et al. 2023), the EV developers have focused on optimizing key components to ensure high energy efficiency in all drive system components, as well as increasing the overall cost-effectiveness of the powertrain. This has favored electrical traction machines (e-machines) with high power density (W/kg and W/L). As a result, synchronous machines with permanent magnets (PMSM) containing rare-earth elements (REEs), typically neodymium (Nd) and, to some extent, dysprosium (Dy), stand out as the most widely used e-machine type in EVs (Cao et al. 2021).

However, when environmental concerns are included among the trade-offs in designing e-machines for EVs, greater consideration is required to balance competing design choices. For instance, high-grade materials used in windings and electric steel – such as copper (Cu) combined with hair-pin winding technique and cobalt-containing electrical steel – can enhance performance but may also result in higher costs and greater environmental impacts compared to conventional design choices. Similarly, optimizing e-machines for efficiency can reduce operational energy demand but may require advanced cooling systems or specialized materials – adding complexity and cost to the design, while the overall environmental impacts remain uncertain. Therefore, quantifying these trade-offs is essential to ensure both relevant technical performance and environmental sustainability throughout the entire lifecycle of the e-machine.

Life cycle assessment (LCA) is used for quantifying and evaluating environmental impacts, and it is especially useful in analyzing trade-offs and hotspots among different technical options intended for the same application. In previous work (Nordelöf et al. 2019), performed an LCA study on three traction machines with different permanent magnets. One of them was a PMSM with neodymium-dysprosium-iron-boron (Nd(Dy)FeB) magnets, and one of the others was a permanent magnet-assisted (PMA-) synchronous reluctance machine (SynRM) with strontium-ferrite magnets. The study showed that although the PMSM with Nd(Dy)FeB-magnets was the lightest and had the highest power density, its toxicity and climate change impacts were the highest among the three options. The main contributor to climate change impacts was the drive-cycle losses. In contrast, the PMA-SynRM traded a lower power density for a higher drive-cycle efficiency, yielding a better overall

environmental performance. The study also concluded that the production of Cu windings, aluminum (Al) housing, and electrical steel sheets indicates a more significant environmental impact than the REE-magnets. The main environmental hotspot for Cu windings was attributed to the extraction of virgin metal, while for electrical steel sheets, they were greatly enhanced by the high material loss rate during e-machine production.

However, global availability of REE materials is uncertain due to geopolitical constraints in combination with the expected rapid demand growth for EVs (IEA 2023a). Thus, this makes it meaningful and obliging to also assess the environmental impact of e-machine alternatives without any magnets. One popular design is the induction machine (IM), which has been used in the Tesla Model S and Audi e-Tron as the main propulsion e-machine (Thomas et al. 2021). These IMs have worse performance in terms of weight and efficiency compared to the REE-equipped PMSMs on the market (Han et al. 2009; Pellegrino et al. 2012). Nevertheless, this performance reduction can be kept to an acceptable level if the IM is allowed to become larger than its PMSM alternative.

Only a few LCA studies on IMs are available in the literature. For example, Schillingmann et al. (2021) compared the environmental impact of manufacturing four types of e-machines with a 100 kW output: a PMSM, an IM, a SynRM, and an electrically excited synchronous machine (EESM). They concluded that the SynRM was the most sustainable option due to its minimal use of Cu and REE magnets, based on midpoint results for climate change impacts, as well as endpoint results in ecosystem quality, human health, and resource availability. However, the use phase was not considered in the study, which limits the overall applicability of the results. Additionally, the study lacks a detailed comparison of the mechanical performance of the three e-machines. Unfortunately, relatively few technical details of the studied machines are publicly available, making it difficult for the reader to link them with the resulting environmental impact. Cassoret et al. (2019) conducted a comparative LCA on an Al-rotor IM and a Cu-rotor IM, revealing that despite the Al-rotor IM having lower manufacturing impacts, the use phase significantly affected the environmental burden, making it a worse option in the end. Similarly, Rassölkin et al. (2020) compared an Al-rotor IM, a SynRM, and a PMA-SynRM with REE magnets, concluding that despite the highest economic cost for the PMA-SynRM, it remained the most energy-efficient option overall, leading to the lowest environmental impact. However, both Cassoret et al. (2019) and Rassölkin et al. (2020) focused on industrial e-machine applications with narrower speed and torque operating ranges than automotive applications. Furthermore, there is a lack of details regarding

the designs and the inventory data in the abovementioned studies, which hinders other studies from developing these scopes further in future studies.

The specific contribution of the work presented in this article is that it expands the scope of LCA investigation to cover three previously unexplored IM variants, each featuring different combinations of stator and rotor windings: an IM with distributed Cu stator windings and Cu rotor bars, an IM with distributed Cu stator windings and Al rotor bars, and an IM with distributed Al stator windings and Al rotor bars. For all IM options, the main geometrical and dimensional data are provided, and so are their speed-torque efficiency and performance maps. By applying the same LCA methodology as Nordelöf et al. (2019), this study maintains consistent performance targets, including current density, maximum torque, and maximum speed, while allowing other parameters, such as high-speed performance and axial length, to vary. This focused approach helps narrow the design-variable space, facilitating a more well-defined assessment of environmental impacts. Furthermore, this research introduces new inventory data for LCA modelling of rotor manufacturing, specifically addressing Al and Cu rotors in IMs, and accounts for additional operational energy consumption due to an increased rotor cooling demand in IMs compared to PMSMs. By offering a detailed LCA comparison of the reference PMSM from the Nordelöf et al. (2019) study and three newly designed IMs, the study aims to provide new insights about the environmental trade-offs involved in e-machine design for EVs. Additionally, in response to questions raised in Nordelöf et al. (2019), this work also explores the climate change impacts of sourcing virgin Al from different origins and the benefits of reducing electrical steel sheet scrap rates during core lamination punching, referred to as a “green manufacturing” scenario.

A supplementary report (SR) provides additional details about the basic principles of IMs, manufacturing procedures, design options, the use phase evaluation, and complete impact assessment results. This information is provided with a high level of transparency in order to make the research reproducible and enable quality assessment. Any figures and tables labelled with an “S” correspond to those found in the SR.

**Table 1** Performance parameters of EV

Parameters	Value	Unit
Curb and driver weight	1,575	kg
Top speed	145	km/h
Total driven distance	200,000	km

## 2 Methods, goal and scope

### 2.1 Goal definition

The goal of this LCA study is to investigate how the choices of stator winding materials and rotor configuration affect the environmental impact of EV propulsion e-machines. A main objective is to support the development and manufacturing of vehicular electric traction systems, or those companies interested in purchasing such ones. This information can aid in balancing requirements at the component level and guide the selection of EM type for the powertrain level. Additionally, the study is relevant to government agencies and academic researchers interested in the environmental impact of automotive technology.

### 2.2 Objects of study and functional unit

In this study, four e-machine options are compared: (1) a PMSM equipped with distributed Cu stator windings and Nd(Dy)FeB magnets (Ref. PMSM), as described in the previous study (Nordelöf et al. 2019); (2) an IM equipped with distributed Cu stator windings and Cu rotor bars (IM1); (3) an IM equipped with distributed Cu stator windings and Al rotor bars (IM2); and (4) an IM equipped with distributed Al stator windings and Al rotor bars (IM3).

The e-machines were evaluated as single traction machines in the same vehicle, where the main vehicle performance requirements, stated in Table 1, were met with all compared e-machine alternatives.

The “Worldwide harmonized light-duty driving test cycle” (WLTC) is used for the energy consumption evaluation during the use phase. All e-machines are thought of as being equipped with a cooling circuit in their housing and liquid coolant for thermal management. However, the power consumption for the stator cooling is neglected since it is assumed to make the same contribution for all studied machine options. In contrast, the IMs are additionally equipped with a rotor cooling for which the power consumption is estimated and added to the use phase consumption. Moreover, the four traction e-machines were designed to provide the same low-speed maximum torque up to base speed, whereas the maximum torque above base speed consequently differs, resulting in different vehicle high speed acceleration performance. The e-machines have slight variations in their peak power ratings, with the Nd(Dy)FeB PMSM and IM2 having a rating of 100kW, and two IMs having somewhat higher peak torques, 101kW for both IM1 and IM3, respectively. The functional unit is set to one driven kilometer, matching common assumptions made in LCA studies of EVs (Nordelöf et al. 2014).

### 2.3 Type of LCA and system boundaries

This work was conducted using an attributional LCA approach, in line with previous work (Nordelöf et al. 2019). It is a cradle-to-grave study, covering all life cycle stages from mineral extraction to the e-machine end-of-life (EoL). For the EoL stage, the study applied the cut-off approach (Nordelöf et al. 2019), meaning that waste separation and treatment steps were fully accounted for, for all materials disposed of, but recycling flows were only followed to the point where they harmonize with upstream input of secondary recycled raw materials.

Regarding the use phase, each e-machine was examined and compared for one type of vehicle and one representative drive cycle (the WLTC, as stated above). For the background system, i.e. the technical system context of the options studied, version 3.11 of the Ecoinvent database (Weidema et al. 2013, Wernet et al. 2016) was employed, e.g., to model inputs to the e-machine factory, magnet supply chain, use phase, and EoL. For materials, ready-made sub-components, and processing chemicals, global averages were used when available; otherwise, European averages were used. For the energy supply to the magnet supply chain, national Chinese data was used, because, in line with Nordelöf et al. (2019), the magnet production chain is located in China, where over 95% of rare-earth elements are produced (Grohol and Veeh 2023). Additionally, to examine the sensitivity of results on the carbon footprint of the magnet production, a sensitivity analysis is performed.

Two distinct electricity scenarios—the current supply mix in Norway and the European supply mix average—were considered for all electricity supply to the foreground system, i.e., e-machine production, EV charging, and the initial post-used separation process in EoL. Given that the GHG intensity of electricity is decreasing globally (IEA 2024), the idea is that these two scenarios represent a low and a high GHG-intense electricity mix, respectively. Consequently, additional changes in the GHG intensity for the electricity supply over time were then not considered, as it can be argued to already be captured by these two scenarios, despite them originating from different geographical scopes rather than time. Combined with the four technical e-machine options, the two electricity scenarios give eight studied options in total, in the baseline study, i.e., before exploration of green manufacturing, and how sensitive results are to the selection of the magnet supply chain data.

Input data for designs and inventory data unit processes, underpinning the results and conclusions, are expected to be relevant for at least another 10 years. This is estimated despite the fact that Nordelöf et al. (2019) states a 5–7-year validity for the reference PMSM from a 2019 starting point. In fact, the observed continued relevance of the PMSM

reference option indicates that it is established as a dominant design solution that appears to persist over a longer period of time. The same time scope is also deemed valid for the EoL modelling, which corresponds to the current dominant regime where e-machines for passenger cars are typically shredded along with the vehicle, or in specific motor shredders, and where the magnets are lost into other material streams and not recovered. This means that advancements in circular strategies, e.g., such that prolong motor life beyond our assumed lifetime driven distance, or such that lead to more precise EoL disassembly and improved material recovery, could alter our results.

The latest version of ReCiPe 2016 v1.03 package (Huijbregts et al. 2017), the most widely used life cycle impact assessment (LCIA) method (Dong et al. 2021), with both the endpoint and midpoint methods, were used. The endpoint methods were used to identify which midpoint impact categories are most important from an e-machine life cycle perspective. Additionally, to include the most updated characterization factors for global warming potentials, the midpoint method IPCC 2021 (Arias et al. 2021) was applied. Furthermore, the crustal scarcity indicator 2020 (Arvidsson et al. 2020) midpoint method was used to estimate resource use impacts instead of the shorter-term mineral resource use indicator incorporated in ReCiPe 2016 v1.03 package, with the argument that long-term mineral resource availability is an important factor for consideration (Chordia 2022).

The SR, Chapters B–G, contains detailed information on modelling electricity supply and transportation, and the complete results of LCIA methods.

## 3 Inventory analysis

### 3.1 E-machine design description

In this work, three newly designed IMs were modelled and analysed by the same finite element software, ANSYS Maxwell version 2023, but with a later version compared to the previous study (Nordelöf et al. 2019). The resulting essential quantities are given in Table 2 for all four technical options sharing the same maximum torque of 239 Nm and an outer diameter of 200 mm. It is expected that the Ref. PMSM has the lowest weight and smallest volume and causes the lowest use-phase internal energy losses, i.e., the highest operational efficiency.

Effective e-machine design involves minimizing energy loss while simultaneously maximizing power and torque density, amongst other design aspects. In order to reach these objectives, a careful design must be made, with a proper amount of materials and a suitable cooling strategy.

**Table 2** Design summary of investigated electric machines

E-machines	Ref. PMSM	IM1	IM2	IM3
Conductors or magnets in Stator/Rotor	Cu/Nd(Dy)FeB	Cu/Cu	Cu/Al	Al/Al
<b>General data</b>				
Maximum torque [Nm]	239			
Maximum power [kW]	100	101	100	101
Weight [kg]	44.9	59.5	62.9	71.2
	100%	133%	140%	159%
Power density [kW/kg]	2.2	1.7	1.6	1.4
	100%	77%	73%	64%
Stator outer diameter [mm]	200			
Stack length [mm]	127	158	178	218
	100%	124%	140%	172%
<b>Drive cycle energy losses due to electric machines</b>				
Loss per km [Wh/km]	12.9	14.2	14.4	16.3
Life cycle loss [kWh]	2576	2921	3161	3354

For an IM, the magnetic fields of both the stator and the rotor are generated by current-carrying conductors. Hence, a conductor material of higher electric conductivity reduces energy loss and gives a higher margin to increase the current, which in turn enhances the magnetic flux density. This enables a more compact IM to achieve the same torque and power with the same cooling method compared to a lower-conductivity conductor. For a PMSM, its rotor magnetic field comes from Nd(Dy)FeB magnets, resulting in much lower energy losses than the rotor bars in the IM for the same power level. Consequently, the Ref. PMSM is the most compact and has the highest power density among all studied technical options, and IM1 with full Cu conductors performs the best among the three IM variants in terms of size and power density.

As Table 2 states, IM1 is 24% longer and 33% heavier compared to the Ref. PMSM, whereas IM2 and IM3 are 40 and 72% longer, as well as 40 and 59% heavier. Furthermore, IM1 has 23% lower power volumetric density than the PMSM, whereas IM2 and IM3 have 27 and 36% lower, respectively.

In Fig. 1, the primary subparts of IMs are depicted together with the different cross-sections for Cu-bar and Al-bar rotors. Most subparts of the studied e-machines are unchanged from previous work and have been described in detail in Nordelöf et al. (2019) and Nordelöf et al. (2018), including bearings, the housing body with cooling channels, the resolver, the housing endbell with the cover plate for the resolver, the stator with distributed windings, and the terminal block. The subparts that are new in the studied IMs and the design for the hollow-shaft rotor cooling system, include a housing endbell with a coolant collector, the water inner lance, the splined hollow-shaft, and the die-cast rotor subpart, all reported in detail in the SR (Chapter B).

### 3.2 Manufacturing

Upstream raw material data, including virgin and recycled resources, was sourced from Ecoinvent 3.11 Weidema et al. (2013), Wernet et al. (2016). The e-machine production data was taken from the inventory data model presented in previous studies Nordelöf et al. (2019) and Nordelöf and Tillman (2018), but with updates made for the IM versions using information gathered from literature, technical reports, and instructional films, as detailed in SR Sect. B. 2.

Recyclable scrap generated during various processes was modelled to be transported to a recycling center, and it is then cut off from the life cycle as burden-free, in line with the overall modelling approach for EoL. This means that all studied e-machine options draw the benefit of having various recycled content brought into the upstream material processing, but then, on the other hand, carry the burdens of producing and processing all extra material lost as scrap during production. The inclusion of recycled content in the upstream material processing helps reduce the environmental impact and the cost of raw materials. However, use of excess material is still burdensome, and the largest source of steel scrap in the manufacturing step is the one-piece punching process, which punches out the desired pattern from the same steel sheet in one stroke (Nordelöf and Tillman 2018). The masses of scraps within the e-machine factory for the four different e-machines are listed in Table 3, shown in kg, and the percentage of the weight of material input to the e-machine factory. It can be seen that the amount of scrap from steel sheet punching increases with the machine volume, and around 30% of the total sheet mass is wasted. For the Cu scrap, IM1 has the highest amount due to the Cu rotor die-casting process (Schiesser et al. 2010).

The SR further explains the different manufacturing steps and detailed schematics illustrating the manufacturing life

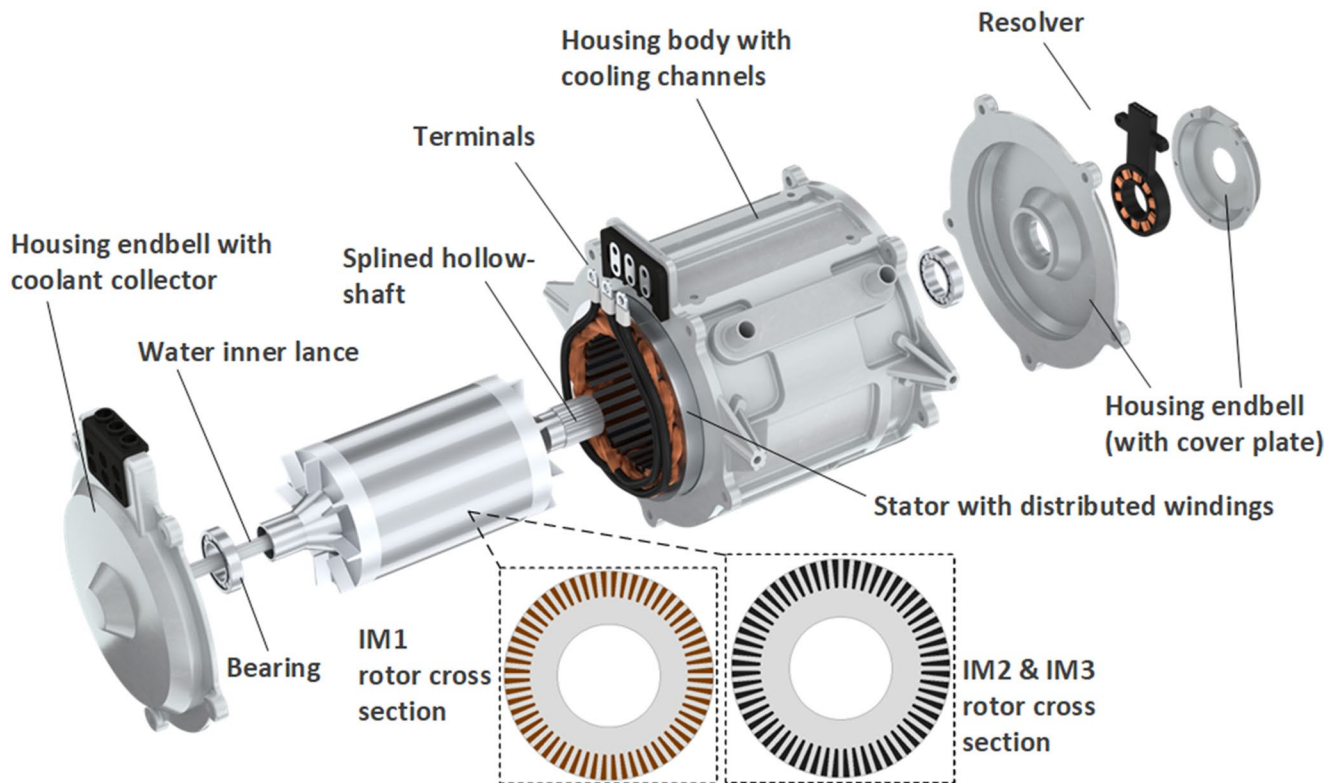


**Fig. 1** Exploded view of the primary design common for all three IM options, including how the rotor laminates differ in their cross sections, with the layout of the IM options – IM1 with Cu conductors in both

stator and rotor, IM2 with Cu stator winding and Al rotor bars, and IM3 with Al conductors in both stator and rotor

**Table 3** Mass of main scraps from the e-machine factory

E-machines	Scraps of steel sheet		Scraps of Al and Cu	
	[kg]	[%]	[kg]	[%]
Ref. PMSM	19.7	30%	0.92	1%
IM1	23.7	28%	3.28	4%
IM2	26.2	30%	1.23	1%
IM3	32.4	32%	1.33	1%

cycle for each of the three IM options can be found in Figs. S2 and S3.

### 3.3 Use phase

To ensure comparability between the IM options and the Ref. PMSM, all energy consumption that is caused by the e-machine, i.e., the energy to overcome e-machine-related losses, including those coupled to its mass contribution in terms of rolling resistance, during the use phase was estimated using the same schematic as in the prior work by Nordelöf et al. (2019). This approach involved applying the standard drive cycle to the efficiency maps of the technical options. Only the surplus energy consumption caused by the losses of e-machines is counted and listed in Table 2. The

same passenger car and powertrain model reported in the SR of Nordelöf et al. (2019) was utilized in this study.

The key update in this work compared to earlier is the inclusion of additional energy consumption due to the rotor hollow-shaft cooling system. This extra consumption is attributed to (1) the extra power required for the cooling pump due to the hollow-shaft cooling path and (2) friction losses from seals designed to prevent coolant leakage into the stator windings. Further details on the additional energy consumption caused by the rotor hollow-shaft cooling system are provided in SR Sect. D.

## 4 Results and discussion

### 4.1 GHG intensity of electricity scenarios

First, as the two electricity scenarios are applied to assess how the GHG intensities of the electricity mixes influence the LCA results, it is relevant to report quantified results for the electricity input in the two scenarios. Both are presented as the average output from the low-voltage grid, including the losses in the charging equipment: the high GHG intensity scenario results in 377 g CO<sub>2</sub>-Eq/kWh (representing the average for European countries) and the low GHG intensity

scenario results in 34 g CO<sub>2</sub>-Eq/kWh (based on Norway's electricity mix).

## 4.2 Endpoint results for ecosystem quality and human health

According to the endpoint indicator results (presented in the SR Chapter G1), climate change and terrestrial acidification are the two midpoint impact categories that contribute most to the total results for ecosystem quality. Eutrophication, water use, land use, terrestrial ecotoxicity, freshwater ecotoxicity, marine ecotoxicity, and photochemical oxidant formation all make minor contributions to the ecosystem quality measure, with variations depending on the electricity scenario. For example, eutrophication gives a notable contribution under the high GHG intensity electricity scenario due to the relatively high reliance on fossil fuels. In contrast, it becomes negligible in the low GHG intensity scenario, attributed to the significant share of hydropower in the electricity mix used in this study. For the human health endpoint impact indicator, the primary contributors are climate change, non-carcinogenic human toxicity, and particulate matter formation.

The key midpoint indicator results are presented in Fig. 2(a)–(e). Figures 2(a)–(c) depict the indicators for non-carcinogenic human toxicity potential, particulate matter formation potential, and terrestrial acidification potential, respectively. Figure 2(d) represents crustal scarcity potential, while Fig. 2(e) illustrates global warming potential. These results are presented with contributions from six different stages in the life cycles of the e-machine options: (1) use phase, (2) Al housing production, (3) electrical steel sheet production, (4) conductor production, (5) the rest of the productions, transport, and EoL and (6) magnet production (only in Ref. PMSM).

The use phase includes the electricity needed to compensate for the losses of each e-machine option during operation, considering their mass and efficiency. The grouped results for the production of the Al housing, electrical steel sheets, and conductors account for all emissions and resource use from the raw material extraction to the factory gate of manufacturing in Europe. Magnet production encompasses the fabrication of magnets in China and their transportation to Europe. The remaining group covers all other components' production, the e-machine assembly factory, EoL activities, and all remaining transports taking place within Europe.

Modified life cycle results for the e-machine options with improved outcomes when applying the two proposed strategies to reduce GHG emissions, using green Al undergone smelting with renewable energy sources or an improved laminate punching, are depicted in Figs. 2(f) and 3.

## 4.3 Results for local and regional impacts, and resource depletion

As shown in Fig. 2(a)–(d), the production of Cu conductors causes substantial impacts across both electricity scenarios on several indicators: non-carcinogenic human toxicity, particulate matter formation, terrestrial acidification, and metal and mineral use in terms of crustal scarcity. This activity and its upstream supply chain release sulfur dioxide, thereby contributing to particulate matter and acidification, and also generate sulfidic tailings containing heavy metals like arsenic, zinc, and Cu, increasing the risk of non-carcinogenic human health issues (Samecka-Cymerman and Kempers 2004). Furthermore, Fig. 2(d) highlights that increased Cu usage significantly elevates the scarcity potential of materials for the e-machine. As a result, the IM1 e-machine design, which utilizes Cu conductors both in the stator and rotor, is identified as the least favorable option in terms of carcinogenic human toxicity, particulate matter formation, terrestrial acidification, and crustal scarcity. It is also worth noting that the risk for crustal scarcity varies significantly between the two electricity scenarios for the use phase, in terms of fossil resources, due to the use of lignite and hard coal in thermal power electricity generation in European countries.

## 4.4 Results for contributions to climate change

In the results for potential climate change impacts, shown in Fig. 2(e), IM3 exhibits the highest contributions in both electricity scenarios. Under the high GHG-intensity electricity scenario, the use phase is the dominant contributor to emissions. However, in the low GHG intensity scenario, emissions are more significantly influenced by the production of Al housing and the electrical steel sheets due to their substantial mass shares in the e-machines, 30%–36% for the former, and 45%–52% for the latter (SR Chapter C2). In contrast, the Nd(Dy)FeB magnets are not identified as a significant contributor to GHG emissions due to their relatively small mass share around 3%, in line with (Nordelöf et al. 2019).

The main source of emissions in the supply chain of the Al housing is the production of primary Al from alumina, which is an electricity-based process that, at some production sites, generates this electricity locally using large amounts of fossil fuels. In the current European market mix for primary Al ingots, such fossil-based routes push up average GHG emission levels. For electrical steel sheets, the main contributor of GHG emissions is primary steel production, which is carried out using blast furnace ovens. These ovens operate around 1500°C to convert iron ore into steel and can release up to three tons of CO<sub>2</sub> per ton of steel produced (IEA 2023b). Additionally, the punching process

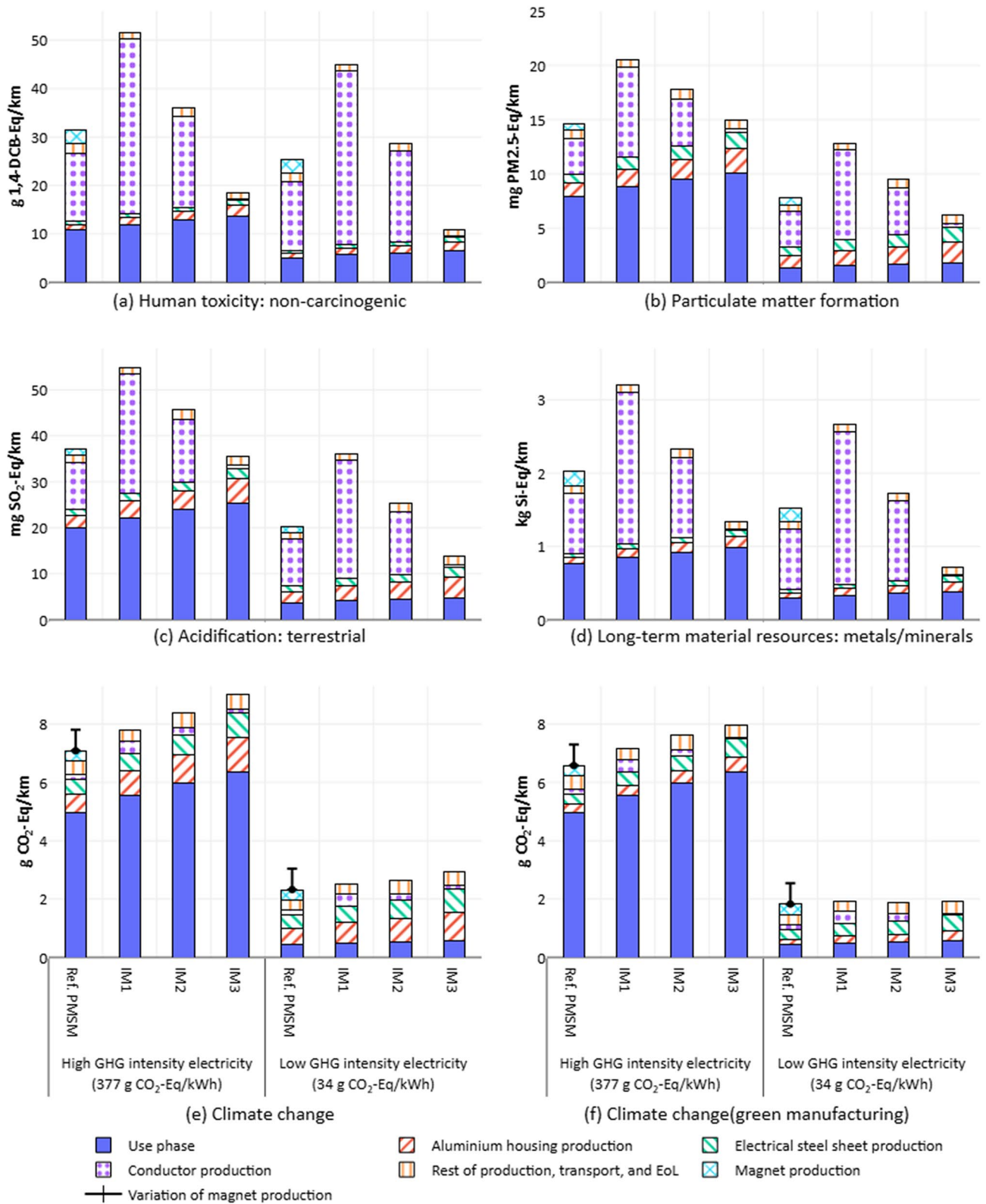
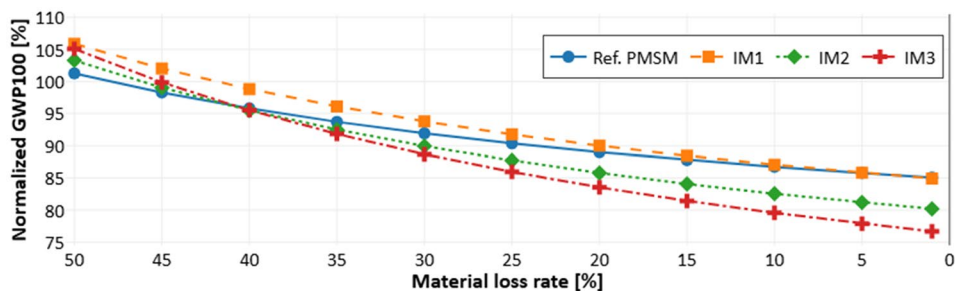


**Fig. 2** Midpoint results for five impact categories with high and low GHG intensity in electricity production, including sensitivity of climate impact to PM production indicated by error bars on Ref. PMSM

**Fig. 3** Midpoint climate change impact reduction potential for e-machine due to a reduced material loss rate after steel sheet punching, indicating braking points for IM2 and IM3 compared to the Ref. PMSM at 40% loss rate



required to produce the sheets for the stator and rotor core stacks contributes significantly to amplifying these emissions. This process has a material loss rate of 48% of input electrical steel (Nordelöf et al. 2019), resulting in substantial scrap generation, as detailed in Table 3. Consequently, around 2 kg of electrical steel sheet is needed to produce 1 kg of machine iron core.

#### 4.5 Results for approaches to reduce climate change impacts

Two major hotspots for GHG emissions in the manufacturing stage were identified: the production and supply chains of the Al housing and electrical steel sheets. This study proposes two strategies to mitigate the emissions associated with these hotspots.

The GHG emissions caused by the Al housing are primarily due to the use of fossil-based electricity when producing virgin Al ingots, even though these, on average, only make up 26% of the raw material input for the Al housing, and most of the input comes from recycled content. To address this, it is recommended to switch this input stream to one relying on less GHG-intensive processing, for instance, using local hydropower-based electricity for virgin Al ingot production. As shown in Fig. 2(f), a change like this could result in a reduction of more than 50% in GHG emissions from the Al housing production.

As highlighted in the previous section, the laminate punching process results in significant amounts of scrap. To address this issue, the second GHG reduction strategy involves improving the punching process through the usage of segmented electrical steel sheet laminations in the e-machine construction. This technique shifts the punching pattern from one complete cross-section into smaller sections, thereby reducing the material loss rate of electrical steel sheets. In Fig. 3, the x-axis shows the material loss rate, and the y-axis shows the normalised global warming potential of e-machine production in relation to the GHG emissions of the Ref. PMSM has approximately 1.35 g CO<sub>2</sub>-Eq/km at a 48% material loss rate. As shown in Fig. 3, a lowered material loss rate can lead to a notable reduction in GHG emissions from the e-machine production. It is

particularly noteworthy that when the material loss rate is reduced to below 40%, the GHG emissions across all technical options are potentially lower than those of the original Ref. PMSM. In practice, the use of segmented laminations implies that sets of smaller sections are first stacked separately and joined by welding, and then also assembled by welding to complete rotor and stator cores. This is different from the original model, which accounts for the assembly welding of stator cores and the pressing of rotor cores onto the shaft. However, even if we assume that the total length of welding joints becomes fifty times longer for segmented laminates, this change has a negligible effect on total e-machine results.

As shown in Fig. 2(f), combining the use of green Al and improving the loss rate down to 25% through segmented lamination could result in a reduction of 24%–44% in GHG emissions from total e-machine production. Furthermore, in such a scenario, the differences in total life-cycle GHG emissions are around 0.1 g CO<sub>2</sub>-Eq/km for the three IM options from the Ref. PMSM, when all are charged with low GHG intensity electricity.

#### 4.6 Sensitivity to the magnet supply chain data for the reference machine

The magnet supply chain LCI model in this study is based on Nordelöf et al. (2019), which originally relied on Eco-invent data for rare-earth oxide (REO) concentrate (70% purity), and included updates for energy use and economic allocation of burdens to Nd and Dy based on REE price data from 2014 to 2016. Since the 3.11 version of Eco-invent is used in this study, rather than the 3.3 version in Nordelöf et al. (2019), there is a notable increase in emissions from 64 to 72 kg CO<sub>2</sub>-eq per motor. In addition, Nordelöf and Bongards (2025) applied economic allocation on REE price data from 2021 to 2024 to two REO supply routes in a cradle-to-gate LCA of PMSMs in EVs, where the choice of supply route accounted for approximately 90–170 kg CO<sub>2</sub>-eq per motor (22–35% of total motor production emissions). These findings highlight the significant uncertainty associated with magnet production.

Furthermore, a review study by Schreiber et al. (2021) identifies that several LCA studies covering the extraction and production of REOs from raw ore were published between 2016 and 2020, and that these studies display large discrepancies in terms of greenhouse gas intensity per kg of pure REO produced. Across different ore types, the variation is almost a factor of five, and the studies underpinning the Ecoinvent datasets for REEs are generally at the lower end (Schreiber et al. 2021). Allocation based on economic value then further amplifies these differences (Nordelöf et al. 2019), but as other constituents than REEs are also present in the magnets, this is to some degree balanced back on the magnet level. Nevertheless, this calls for an investigation of how sensitive the results are to the selection of magnet supply chain data.

To investigate what effect the variation pointed out by Schreiber et al. (2021) would have on the results of this study, a sensitivity analysis was conducted using the original dataset as a baseline and increasing the GHG emissions from the magnet supply chain by 100 and 200%, respectively. Detailed outcomes are presented in SR Chapter G and visualized as whisker plots for the 200% increase in Fig. 2(e) and (f). The results indicate that the Ref. PMSM continues to exhibit the lowest global warming potential when the EV is charged using electricity with high GHG intensity, even under the most extreme emission scenario for the magnet supply chain. In contrast, under conditions of low GHG intensity electricity, and the application of green manufacturing practices, all IM alternatives become comparable to the Ref. PMSM in terms of global warming potential.

## 5 Concluding implications for e-machine design and material usage

Given its high efficiency across a broad operating range and excellent power density, the Ref. PMSM with Nd(Dy)FeB magnets causes the lowest GHG emissions among the four e-machine options, regardless of the electricity mix. However, if the improvement approach to select green virgin Al is applied, all four e-machine options become roughly comparable in terms of GHG emission in the low GHG intensity electricity scenario. When the broader range of impact categories is considered, IM3 with full Al conductors emerges as the best-performing option. This configuration delivers favorable results across several categories, including non-carcinogenic human toxicity, particulate matter formation, and resource scarcity.

Consistent with the findings from previous studies (Nordelöf et al. 2019), the baseline results indicate that the magnet production and its supply chain are not a significant source of GHG emissions for the PMSM e-machine option,

but this is due to its relatively low mass share, and not because of low emission intensity. However, the sensitivity analysis shows that other, more emission intensive data for the magnet supply chain could subvert this observation, at least in a low carbon intensity setting as regards the charging electricity. Still, the energy losses of the e-machines during operation remain a primary contributor to GHG emissions and the climate change impact category, particularly when they are powered by high GHG intensity electricity. For the low GHG scenario, it is the production of Al housings and electrical steel sheets that becomes most important for all IM options and the baseline version of the reference PMSM. Choosing Al produced using renewable electricity, or increasing the share of recycled Al, could significantly reduce the emissions linked to the Al housing production. By decreasing the material loss rate in the LCA study for the steel sheet punching, the results indicate a potential reduction in the climate change impact. Given the observed variability and the influence of the chosen REE supply route, we recommend that sensitivity analysis be conducted in studies of EV traction e-machine LCA when REE magnets are used. This practice would ensure that conclusions remain robust under different assumptions and data sources.

For human toxicity impacts and long-term resource scarcity, the production of Cu conductors is the main source of impact. To address this, it is recommended to increase the use of secondary Cu and explore alternative conductor materials or techniques that minimize Cu usage. For instance, Al hairpin windings could compensate for the efficiency loss that occurs when switching to Al, while reducing the need for Cu (Cutuli et al. 2022). Otherwise, given that the demand for virgin Cu is expected to continue to increase (Schipper et al. 2018), it is also important to improve current Cu mining processing, and specifically, the mining waste handling.

## 6 Future work

To further advance knowledge regarding the environmental impact of the life cycle of the studied electric machines, several areas for future research have been identified.

It would be valuable to evaluate the use-phase energy consumption during different operating temperatures, such as driving in cold and warm climates. In this study, thermal aspects are considered in terms of a set (and relatively high) operating temperature for both the conductor and magnet. In an extended study of the impact of operating temperature, higher-order thermal models are recommended, e.g., conjugate heat transfer models. Such models can also capture the effect of internal thermal gradients during operation as well as the impact of the cooling system and its contribution to total energy consumption.

Additionally, a more detailed loss model that accounts for the different topologies of segmented laminations and their impact on iron loss would also be a highly valuable subject for further research.

Furthermore, the current modelling of rotor cooling in IMs includes only pump power and seal friction losses. A more comprehensive treatment should account for system complexity, leakage risks, and maintenance demands to avoid underestimating environmental and operational impacts.

Extending this study by incorporating differentiated durability assumptions based on empirical reliability data would be highly valuable. In particular, IMs with AI windings or bars may exhibit shorter lifetimes due to thermal and mechanical stress, such as joint integrity, thermal expansion, and vibration resistance (Hodowanec and Finley 2002; Knych et al. 2025), which could significantly affect life cycle outcomes. It would be beneficial to reflect on the performance and durability in the real world to integrate these factors.

Finally, expanding the life cycle scope to include more advanced EoL scenarios, such as component re-use or remanufacturing, or more detailed modeling of recycling, would bring valuable new insights regarding the environmental impact of e-machines.

**Supplementary Information** The online version contains supplementary material available at <https://doi.org/10.1007/s11367-026-02610-7>.

**Funding** Open access funding provided by Chalmers University of Technology.

**Data availability** The authors declare that the data supporting the findings of this study are available within the paper, the previous studies (Nordelöf and Tillman 2018; Nordelöf et al. 2018, 2019), and their supplementary reports.

## Declarations

**Competing interests** The authors declare no competing interests.

**Open Access** This article is licensed under a Creative Commons Attribution 4.0 International License, which permits use, sharing, adaptation, distribution and reproduction in any medium or format, as long as you give appropriate credit to the original author(s) and the source, provide a link to the Creative Commons licence, and indicate if changes were made. The images or other third party material in this article are included in the article's Creative Commons licence, unless indicated otherwise in a credit line to the material. If material is not included in the article's Creative Commons licence and your intended use is not permitted by statutory regulation or exceeds the permitted use, you will need to obtain permission directly from the copyright holder. To view a copy of this licence, visit <http://creativecommons.org/licenses/by/4.0/>.

## References

- Arias P, Bellouin N, Coppola E, Jones R, Krinner G, Marotzke J, Naik V, Palmer M, Plattner G-K, Rogelj J, Rojas M, Sillmann J, Storelvmo T, Thorne P, Trewin B, Achuta Rao K, Adhikary B, Allan R, Armour K, Bala G, Barimalala R, Berger S, Canadell J, Cassou C, Cherchi A, Collins W, Collins W, Connors S, Corti S, Cruz F, Dentener F, Dereczynski C, Di Luca A, Diongue Niang A, Doblans-Reyes F, Dosio A, Douville H, Engelbrecht F, Eyring V, Fischer E et al (2021) Technical summary. Cambridge University Press, Cambridge, United Kingdom and New York, NY, USA, pp 33–144. <https://doi.org/10.1017/9781009157896.002>
- Arvidsson R, Söderman ML, Sandén BA, Nordelöf A, André H, Tillman A-M (2020) A crustal scarcity indicator for long-term global elemental resource assessment in LCA. *Int J Life Cycle Assess* 25:1805–1817
- Cao Z, Mahmoudi A, Kahourzade S, Soong WL (2021) An overview of electric motors for electric vehicles. In 2021 31st Australasian Universities Power Engineering Conference (AUPEC), pp 1–6. <https://doi.org/10.1109/AUPEC52110.2021.9597739>
- Cassoret B, Manata J-P, Mallard V, Roger D (2019) Comparative life cycle assessment of induction machines made with copper-cage or aluminium-cage rotors. *IET Electric Power Appl* 13:712–719. <https://doi.org/10.1049/iet-epa.2018.5401>
- Chordia M (2022) Taking stock of large-scale lithium-ion battery production using life cycle assessment. Chalmers Tekniska Högskola, Sweden
- Cutuli G, Barater D, Nategh S, Raghuraman B (2022) Aluminum hairpin solution for electrical machines in e-mobility applications: Part I: electromagnetic aspects. In 2022 International Conference on Electrical Machines (ICEM), pp 1770–1776. <https://doi.org/10.1109/ICEM51905.2022.9910945>
- Dong Y, Hossain MU, Li H, Liu P (2021) Developing conversion factors of lcia methods for comparison of lca results in the construction sector. *Sustainability* 13. <https://www.mdpi.com/2071-1050/13/16/9016>. <https://doi.org/10.3390/su13169016>
- Forsythe CR, Gillingham KT, Michalek JJ, Whitefoot KS (2023) Technology advancement is driving electric vehicle adoption. *Proc Natl Acad Sci India Sect B Biol Sci* 120(23):e2219396120. <https://doi.org/10.1073/pnas.2219396120>, <https://www.pnas.org/doi/abs/10.1073/pnas.2219396120>, <https://www.pnas.org/doi/pdf/10.1073/pnas.2219396120>
- Grohol M, Veeh C (2023) Study on the critical raw materials for the EU 2023. Publications Office of the European Union. <https://doi.org/10.2873/725585>
- Han P-W, Chun Y-D, Choi J-H, Kim M-J, Koo D-H, Lee J (2009) The study to substitute aluminum for copper as a winding material in induction machine. In INTELEC 2009 - 31st International Telecommunications Energy Conference, pp 1–3. <https://doi.org/10.1109/INTLEC.2009.5352008>
- Hodowanec M, Finley WR (2002) Copper versus aluminum induction-motor rotors: which construction is best? *IEEE Ind Appl Mag* 8(4):14–25. <https://doi.org/10.1109/MIA.2002.1011184>
- Huijbregts MA, Steinmann ZJ, Elshout PM, Stam G, Verones F, Vieira M, Zijp M, Hollander A, Van Zelm R (2017) Recipe2016: a harmonised life cycle impact assessment method at midpoint and endpoint level. *Int J Life Cycle Assess* 22:138–147
- IEA (2023a) Road transport. Technical report. IEA. <https://www.iea.org/reports/road-transport>
- IEA (2023b) Steel. <https://www.iea.org/energy-system/industry/steel>
- IEA (2023c) Tracking clean energy progress 2023. Technical report. <https://www.iea.org/reports/tracking-clean-energy-progress-2023>, IEA

- IEA (2024) Executive summary – electricity 2024. Technical report. IEA. <https://www.iea.org/reports/electricity-2024/executive-summary>
- IPCC (2023) Transport. Cambridge University Press, pp 1049–1160
- Knych T, Smyrak B, Jurkiewicz B (2025) A comparative analysis of the fatigue strength of aluminium and copper wires used for power cables. *Materials* 18. <https://doi.org/10.3390/ma18184426>, <https://www.mdpi.com/1996-1944/18/18/4426>
- Nordelöf A, Bongards A (2025) Allocating the environmental burdens in co-production of rare earth elements for EV magnets. In EVS38 International Battery, Hybrid and Fuel Cell Electric Vehicle Symposium, 2025. <https://vti.diva-portal.org/smash/record.jsf?pid=diva2%3A1973021%26dswid=2248>
- Nordelöf A, Grunditz E, Lundmark S, Tillman A-M, Alatalo M, Thiringer T (2019) Life cycle assessment of permanent magnet electric traction motors. *Transp Res Part D Transp Environ* 67:263–274. <https://doi.org/10.1016/j.trd.2018.11.004>
- Nordelöf A, Messagie M, Tillman A-M, Ljunggren Söderman M, Van Mierlo J (2014) Environmental impacts of hybrid, plug-in hybrid, and battery electric vehicles—what can we learn from life cycle assessment? *Int J Life Cycle Assess* 19:1866–1890. <https://doi.org/10.1007/s11367-014-0788-0>
- Nordelöf A, Poulidikou S, Chordia M, Bitencourt de Oliveira F, Tivander J, Arvidsson R (2019) Methodological approaches to end-of-life modelling in life cycle assessments of lithium-ion batteries. *Batteries* 5. <https://www.mdpi.com/2313-0105/5/3/51>
- Nordelöf A, Tillman A-M (2018) A scalable life cycle inventory of an electrical automotive traction machine—Part II: manufacturing processes. *Int J Life Cycle Assess* 23:295–313. <https://doi.org/10.1007/s11367-017-1309-8>
- Nordelöf A, Tillman A-M, Grunditz E, Thiringer, Torbjörn M, Alatalo M (2018) A scalable life cycle inventory of an electrical automotive traction machine—Part I: design and composition. *Int J Life Cycle Assess* 23:55–69. <https://doi.org/10.1007/s11367-017-1308-9>
- Pellegrino G, Vagati A, Boazzo B, Guglielmi P (2012) Comparison of induction and pm synchronous motor drives for EV application including design examples. *IEEE Trans Ind Appl* 48(6):2322–2332. <https://doi.org/10.1109/TIA.2012.2227092>
- Rassölkin A, Belahcen A, Kallaste A, Vaimann T, Lukichev V, Orlova S, Heidari H, Asad B, Pando J (2020) Life cycle analysis of electrical motor-drive system based on electrical machine type. *Proc Est Acad Sci*. <https://api.semanticscholar.org/CorpusID:219482064>
- Samecka-Cymerman A, Kempers A (2004) Toxic metals in aquatic plants surviving in surface water polluted by copper mining industry. *Ecotox Environ Safe* 59(1):64–69. <https://www.sciencedirect.com/science/article/pii/S0147651303002288>
- Schiesser P, Jaouen N, Martin J-B, Dupuis D, Verlant D, Dovergne F (2010) Analyse de cycle de vie comparative entre deux moteurs électriques. Technical report, Écoeff. and FAVI
- Schillingmann H, Gehler S, Henke M (2021) Life cycle assessment of electrical machine production considering resource requirements and sustainability. In 2021 11th International Electric Drives Production Conference (EDPC), pp 1–7
- Schipper BW, Lin H-C, Meloni MA, Wansleben K, Heijungs R, van der Voet E (2018) Estimating global copper demand until 2100 with regression and stock dynamics. *Resour Conserv Recy* 132:28–36. <https://www.sciencedirect.com/science/article/pii/S0921344918300041>
- Schreiber A, Marx J, Zapp P (2021) Life cycle assessment studies of rare earths production - findings from a systematic review. *Sci Total Environ* 791:148257. <https://www.sciencedirect.com/science/article/pii/S0048969721033283>
- Thomas R, Husson H, Garbuio L, Gerbaud L (2021) Comparative study of the tesla model s and audi e-tron induction motors. In 2021 17th Conference on Electrical Machines, Drives and Power Systems (ELMA), pp 1–6. <https://doi.org/10.1109/ELMA52514.2021.9503055>
- Weidema B, Bauer C, Hischer R, Mutel C, Nemecek T, Reinhard J, Vadenbo C, Wernet G et al (2013) The ecoinvent database: overview and methodology, data quality guideline for the ecoinvent database version 3. Ecoinvent Center, Zürich. Retrieved (Der folgende Link führt zur zuvor genannten Veröffentlichung: <https://www.ecoinvent.org>)
- Wernet G, Bauer C, Steubing B, Reinhard J, Moreno-Ruiz E, Weidema B (2016) The ecoinvent database version 3 (Part I): overview and methodology. *The Int J Life Cycle Assess* 21:1218–1230. <https://doi.org/10.1007/s11367-016-1087-8>

**Publisher's Note** Springer Nature remains neutral with regard to jurisdictional claims in published maps and institutional affiliations.